wPMLG-5 Spectroscopy of self-aggregated BChl e in natural chlorosomes of Chlorobaculum limnaeum

Miloslavina, Y.; Sai Sankar Gupta, K.B.; Tank, M.; Bryant, D.A.; Groot, H.J.M. de

Full Paper

Israel Journal of Chemistry

DOI: 10.1002/ijch.201300129

wPMLG-5 Spectroscopy of Self-Aggregated BChl *e* in Natural Chlorosomes of *Chlorobaculum Limnaeum*

Yuliya Miloslavina,[a] Karthick Babu Sai Sankar Gupta,[a] Marcus Tank,[b] Donald A. Bryant,[b, c] and Huub J. M. de Groot*[a]

In Celebration of Professor Shimon Vega's 70th Birthday

Abstract: ^{1}H magic angle spinning (MAS) nuclear magnetic resonance (NMR), employing rapid spinning and the wPMLG-5 pulse sequence, was used to explore the possibility for performing ^{1}H solid state NMR of a light-harvesting organelle, the chlorosome antenna of *Chlorobaculum limnaeum*. This natural antenna system is built from bacteriochlorophyll *e* (BChl *e*) molecules that are self-assembled to form a supramolecular scaffold for *in vivo* harvesting of light. We present preliminary data on this chlorosome species and address the feasibility of performing wPMLG spectroscopy, in terms of high power irradiation on a fragile biological sample. In parallel, enhancing the ^{1}H shift dispersion from the magnetic field can help to resolve signals from protons that resonate downfield. Different line narrowing mechanisms operating in parallel provide access to resolving selected ^{1}H signals collected from the moderately sized and chemically diverse BChl *e* molecular motif in the chlorosome scaffold. These discoveries will be helpful for future studies of structural and functional characteristics of self-assembled natural and artificial light-harvesting molecules.

Keywords: bacteriochlorophyll *e* · chlorosomes · light-harvesting · MAS NMR spectroscopy · photosynthesis · wPMLG

1 Introduction

Protons (^{1}H) are the most abundant and the most sensitive nuclei for NMR observations. They have the highest gyromagnetic ratio (γ) among all stable isotope species and a convenient relaxation time T_1, which is generally less than a second for organic systems. In addition, hydrogen bonding and aromatic π–π interactions can induce large ^{1}H shifts that are more prominent than for the ^{13}C response, taking into account that the characteristic chemical shift range is ~20 ppm for protons, compared to ~200 ppm for carbons. This makes ^{1}H NMR shift analysis a powerful tool for resolving intermolecular interactions and studying the self-assembly of molecules.[1–4] In the solid state, however, resolving proton signals is not straightforward. The proton spins form a strongly dipolar-coupled network, which induces pronounced overlap and line broadening. Multiple spin dipolar interactions are unfavorable for line narrowing by magic angle spinning (MAS) NMR spectroscopy.[5,6] There are three methods to decrease the ^{1}H linewidth: multiple pulse decoupling, truncation of dipolar interactions by increasing the spinning frequency, and dilution of the ^{1}H network, generally achieved by partial incorporation of deuterium (^{2}H) isotopes. In this short note, we describe the results of studies of the operation of these three mechanisms in parallel for a moderately sized bacteriochlorophyll (BChl) *e* molecule, self-assembled in natural chlorosomes and containing ^{13}C and ^{1}H at natural abundance.

Bacteriochlorophylls are sterically crowded in their side chains and contain many unsaturated carbons in a large macro-aromatic cycle (Figure 1). As a result, the protons are naturally diluted on the ring, while they are abundant in the side chains. Because of the chemical nature of the compound and the unsaturation, the ^{1}H response is partially well dispersed, and the dispersion can be further increased at high magnetic field, with concomitant line narrowing. The reason that we devote this study to the special issue in celebration of Shimon Vega's 70th birthday is that he is one of the pioneers in developing advanced proton line narrowing methods and, in particular, the family of phase-modulated Lee Goldburg (PMLG) techniques, which is widely used in resolving proton signals with MAS NMR.[7–13] To complement the

[a] Y. Miloslavina, K. B. S. S. Gupta, H. J. M. de Groot
Leiden Institute of Chemistry
Einsteinweg 55
2333 CC Leiden (The Netherlands)
e-mail: groot_h@chem.leidenuniv.nl

[b] M. Tank, D. A. Bryant
Department of Chemistry and Molecular Biology
The Pennsylvania State University
University Park, PA (U.S.A.)

[c] D. A. Bryant
Department of Chemistry and Biochemistry
Montana State University
Bozeman, MT (U.S.A.)

Israel Journal of Chemistry

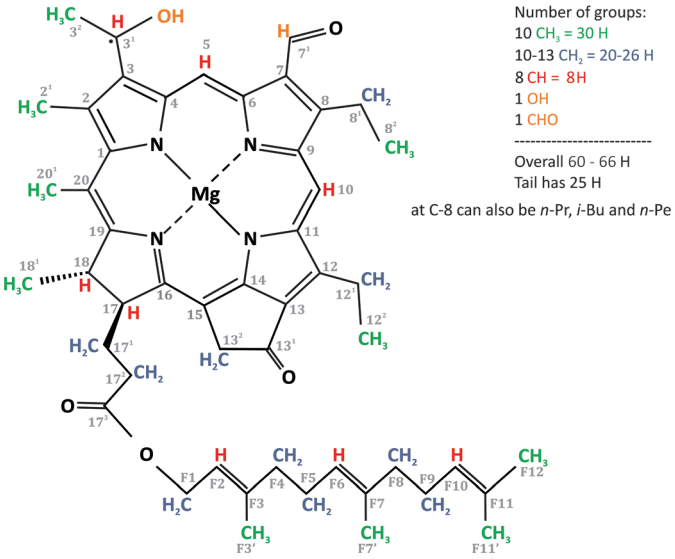

Figure 1. Chemical structure of BChl *e* with all protons marked. The numbering of the macro-cycle is in accordance with the IUPAC convention.[42]

dispersion from high magnetic field and the dilution of the proton network by the unsaturated carbon macro-aromatic cycle, we use the wPMLG-5 decoupling scheme.

2 Experimental Section

2.1 Chlorosome Preparations

Chlorosome isolation was performed as previously described.[14] In brief, cultures of *Chlorobaculum limnaeum* from the strain DSM1677T were harvested after 7 days. Cells were centrifuged (7500 × *g*, 20 min) and were resuspended in a buffer solution (10 mM Tris-HCl, pH 7.5, 2.0 M NaSCN, 5.0 mM EDTA, 1.0 mM PMSF, 2.0 mM DTT). A 3 mg/ml lysozyme solution was added to the cell suspension, which was then incubated at room temperature for 30 min. After that, the cells were mechanically disrupted using a French press at 138 MPa and for at least 3 cycles. Chlorosomes were separated from large cellular debris and unbroken cells by centrifugation (10,000 × *g*, 20 min). The chlorosomes and membrane vesicles in the supernatant were concentrated by ultracentrifugation at 220,000 × *g* for 2 h. The chlorosomes were separated from membranes on a continuous sucrose density gradient with 10–53 % linear gradients prepared in isolation buffer by ultracentrifugation at 220,000 × *g* for 18 h at 4 °C. The chlorosomes were subsequently washed twice with 4 volumes of phosphate buffer (10 mM potassium phosphate, pH 7.2, 150 mM NaCl) and pelleted by ultracentrifugation at 220,000 × *g* for 1.5 h. The isolated chlorosomes were resuspended in 1–2 ml of phosphate buffer containing 1.0 mM PMSF and 2.0 mM DTT and stored at 4 °C until further required.

2.2 wPMLG-5 NMR Measurements

The NMR experiments were performed with an AV-750 (17.6 Tesla) NMR spectrometer equipped with a 2.5 mm triple resonance MAS probe (Bruker BioSpin GmbH, Karlsruhe, Germany). The sample was loaded into a 2.5 mm rotor made from zirconium oxide and was inserted into the MAS probe. The sample was rotated at 30 kHz, and the temperature was set at 277 K. A proton pulse length of 2.1 μs was used for the wPMLG-5 homonuclear decoupling. The phases of the pulses were 20.78, 62.35, 103.92, 145.49, 187.06, 7.06, 325.49, 283.92, 242.35, and 200.78 degrees. The lengths of the magic flip angle and π/2 pulses used for the preparation phase of the wPMLG experiment were 1.0 and 2.1 μs, respectively; the length of the single PMLG pulse was 1.5 μs (Figure 2). The acquisition window was 3.1 μs. The proton on-resonance radiofrequency (rf) field used for PMLG was 100 kHz.

2.3 Derivation of the Scaling Factor

The scaling factor for the wPMLG-5 glycine spectrum was derived from the center point between the two CH_2 signals and the maximum of the NH_2 signal at 3.7 and 8.3 ppm,[15] respectively. The dwell time, corresponding to the acquisition time between two successive data points,

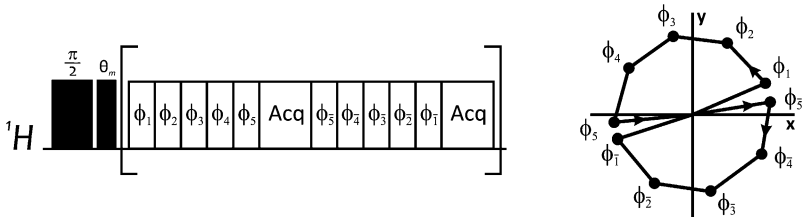

Figure 2. The wPMLG pulse sequence applied in this study (left panel) and corresponding rf pulse trajectories. Following excitation with a π/2 pulse and a pulse at the magic angle, a PMLG train of five pulses is applied, followed by an acquisition window. The phases of the rf pulses are alternated between the first and second halves of the PMLG scheme, according to $\Phi_1 = 20.78°$, $\Phi_2 = 62.35°$, $\Phi_3 = 103.92°$, $\Phi_4 = 145.49°$, $\Phi_5 = 187.06°$, $\Phi_{\bar{5}} = 7.06°$, $\Phi_{\bar{4}} = 325.49°$, $\Phi_{\bar{3}} = 283.92°$, $\Phi_{\bar{2}} = 242.35°$, $\Phi_{\bar{1}} = 200.78°$ to provide the trajectory of the rf pulses during the wPMLG experiment according to the right panel.

was adjusted manually after the experiment has finished, in order to match this difference of 4.6 ppm. The scaling factor was then calculated according to scaling factor = s_dw/(p5+p9), where s_dw stands for the adjusted dwell time, p5 is the length of the PMLG block (7.5 μs), and p9 is one half of the sampling window (2.3 μs). This calculation leads to a scaling factor of 0.6. The same scaling factor was then used to process the BChl *e* wPMLG-5 spectrum.

3 Results and Discussion

BChl *e* is the main light-harvesting pigment in brown-colored, green sulfur, photosynthetic bacteria *Chlorobaculum limnaeum*. The light-harvesting is performed by chlorosomes, oblong bodies which consist of a large amounts of BChls, up to $2.5{\cdot}10^5$ molecules per chlorosome.[16,17] The BChl *e* molecules in the chlorosomes are tightly packed and organized in protein-free, rod-like complexes,[18–20] which results in one of the most efficient light-harvesting and energy transduction structures found in photosynthetic organisms.[21] This allows the bacteria to grow at much lower irradiance levels than other organisms and also provides inspiration for the chemical design of artificial light-harvesting and charge-separation modules. The cells of *C. limnaeum* are rod-shaped and 0.6–0.8 μm wide, and the organism can grow well in non-motile layers of water or sediments rich in reduced sulfur compounds. Under anoxygenic conditions it can use sulfides, polysulfides, elemental sulfur, or molecular hydrogen as electron donors instead of oxygen.[22,23] It is a strict photoautotroph.

BChl *e* was first isolated and structurally characterized by Gloe and co-workers.[24,25] It has a similar structure to BChl *c* and is the only BChl with a formyl group at carbon C7, instead of a methyl group (Figure 1). Similarly to other BChls that are found in nature, BChl *e* exists as different homologs, which vary in their chirality at $C3^1$ (*R*/*S*-epimers), in their C8 and C12 methylated substituents, and in the esterifying alcohol chains at C17.[26–29] Up to 23 homologs were detected,[30] and their relative concentration in a chlorosome depends upon the culture environment. Borrego *et al.*[27] reported that low irradiance leads to the enrichment of highly $C8^2$-methylated BChl *e* homologs. Thus, molecular derivatization and structural variability affects the efficiency of light absorption and energy transfer in the chlorosome. Further development of ^{1}H solid state NMR technology will be helpful in underpinning the self-assembly and organization of BChls in chlorosomes and other BChl-like aggregates.

While, in the past, PMLG decoupling was applied to small molecules for consistent line narrowing of the ^{1}H signals, the purpose of the present study is an initial exploration into improving the proton resolution with PMLG for a more complex and chemically diverse molecule, the BChl *e*, while in its natural chlorosome environment, an organelle of biological origin.

The PMLG sequence builds on the Lee Goldburg (LG)[31] and frequency switched Lee Goldburg (FSLG) sequences that were developed earlier.[32,33] In the LG scheme, a continuous off-resonance rf field is applied at $\omega_{LG} = \omega_1/\sqrt{2}$, where ω_1 is the rf field strength, and the spins rotate around an effective field tilted away from the static magnetic field direction by the magic angle. In the FSLG scheme, the efficiency of decoupling improves if the rf irradiation frequency is switched between the two LG conditions $\omega_{FSLG} = \pm\omega_1/\sqrt{2}$ with a phase shift of π after each 2π rotation of the proton magnetization around the effective field, with the duration of $\tau_{LG} = \sqrt{\frac{2}{3}}\frac{2\pi}{\omega_L}$. In the PMLG sequence, the line narrowing is achieved not by frequency switching, which remains constant, but by applying a burst of rf pulses with well-defined phases that vary sequentially from one pulse to another, rotating the magnetization through the 2π angle in the first half of the rotor cycle around the magic angle and through an angle of −2π in the second half of the cycle.[7]

In this study, we use the PMLG-5 cycle,[10] which approximates an LG unit of 5 on-resonance pulses, each with a duration of $\tau_{LG}/5$ and a phase increment of $\Delta\Phi = 207.8°/2*5$ between successive pulses (Figure 2). At an angle of 207.8°, the rf precesses in one PMLG unit in the rotating frame, and it is equal to $|\omega_{PMLG}|\tau_{LG}$. A constant *rf* power of 100 kHz was used in all the experiments. In the preparation period, the π/2 pulse creates initial magnetization in the plane perpendicular to the direction of the effective field. The magic angle pulse θ_m locks the spins at the magic angle during the PMLG sequence that follows. Previously it was proposed that the combination of π/2 and θ_m would enhance the signal by increasing the averaged magnetization. This combination was used in the first PMLG sequences, in order to make sure that the magnetization is perpendicular to the direction of the effective chemical shift Hamiltonian.[7] The pulse scheme in Figure 2 allows us to explore both a combination of two preparation pulses and a single preparation pulse, and we did not notice an improvement of the signal when both preparatory pulses were used, as opposed to a single π/2 pulse. In this respect, the preparation was also reduced to only one π/2 pulse in recent studies of the Vega group aimed at developing wPMLG sequences further. The preparation period was followed by the wPMLG sequence consisting of a train of pulses with narrow windows for direct acquisition of the signal, resulting in wPMLG-5.[10,13,34]

The implementation of the wPMLG-5 pulse sequence on our spectrometer was first tested on glycine (Figure 3). The three peaks are well resolved, two coming from CH_2 and one from NH_2 groups. The calibration of the spectra was done in such a way that the spectral lines are in agreement with previous works,[12,15] and the proton sig-

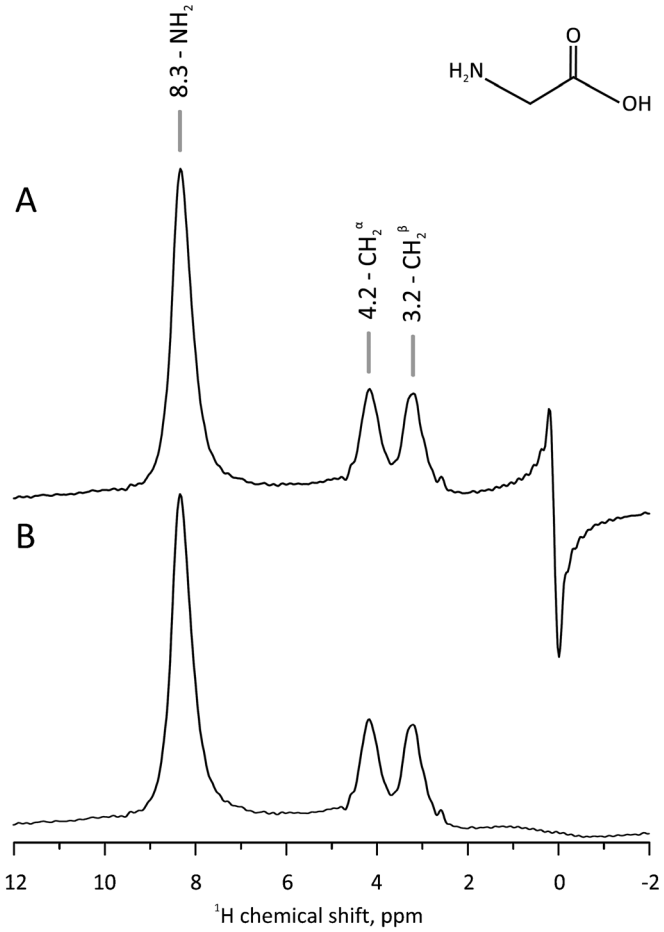

Figure 3. wPMLG of glycine showing the zero frequency artifact (A) and after the qfil baseline correction during data processing (B).

nals are at 3.2, 4.2, and 8.3 ppm. In this way, a scaling factor of 0.6 was found. Figure 3 illustrates how the data processing can handle the zero-frequency artifacts in a wPMLG experiment from pulse imperfections that cannot be removed easily by phase cycling. This allows us to reduce the power and avoid possible heating damage to a fragile biological sample by using a single wPMLG-5 block between acquisition periods. While Figure 3A shows the original spectrum with a strong zero frequency artifact at ~0.5 ppm ^{1}H shift, the spectrum in Figure 3B shows how this artifact was effectively removed by applying a qfil baseline correction,[35] using a Gaussian function with a width of 0.2 ppm. This validates the implementation of the wPMLG on the spectrometer, including the qfil function processing. The sequence performs well, with a residual linewidth of ~0.5 ppm, or 0.4 kHz.

Chlorosomes were maintained in a wet or moist paste-type environment, while PMLG experiments are usually applied to dry solid samples. Figure 4 presents the proton response collected from a sample of BChl *e*-containing chlorosomes with a single $\pi/2$ pulse for two chlorosome preparations. In Figure 4A, the isolated chlorosomes were measured in a water-containing buffer, while in Figure 4B, protons in the buffer were substituted with deuterium. The main water peak occurs at 4.46 ppm, and the signal is much weaker in the deuterated sample. Our earlier MAS NMR studies of chlorosomes from *Chlorobaculum tepidum* showed that NMR signals from chlorosomes are almost exclusively due to the self-aggregated BChls.[17,36] Thus, we attribute the response after deuteration in Figure 4B to the self-assembled BChl *e*, with a minor contribution from the residual H_2O in the buffer. The wPMLG-5 spectrum for the BChl *e* response from the chlorosomes in deuterated buffer is shown in Figure 4C. The qfil function was applied in the same way as for the wPMLG-5 spectrum of glycine (Figure 3). However, it was not possible to remove the zero frequency artifact completely because of complexity of BChl *e* molecule in comparison to glycine. The peak at around −3 ppm and a wave at around 0 ppm come from the artifact, since there are no pronounced peaks in this area in the spectra measured with a single pulse (Figure 4A–B). We have applied the scaling factor of 0.6 that was determined for glycine in the data processing for the BChl *e*. Using this scaling factor, we recover the same separation between the water signal and the aliphatic signal as for the single pulse experiment in Figure 4B, which suggests that the effect of the artifact on the scaling is minor.

The BChl *e* molecule comprises 60–66 protons, depending on the substituents at C8 and C12 (Figure 1). Almost half of those protons are found in the esterifying farnesol group at C17, and 18 protons are in the CH_3 groups. Only a few hydrogens are attached directly to the macro-aromatic ring, namely the meso-protons at positions 5 and 10 and the protons at positions 17 and 18. Resolving the signals from such ring protons can be of interest for structure and structure-function investigations.[4]

Although we cannot assign the BChl *e* shifts only on the basis of proton NMR, we can give a general classification of the signals from their analogy with NMR shifts of BChl *c*, which differs from BChl *e* only in the formyl group at C7, and by comparing with the glycine ^{1}H response in Figure 2. The NMR measurements on BChl *c*-containing chlorosomes were done with ^{13}C labelling, which allowed 2D ^{1}H-^{13}C heteronuclear correlation experiments, as well as homonuclear recoupling and spin diffusion NMR.[37–40] This gives a good basis of ^{1}H-NMR shifts to compare with those obtained for BChl *e* here. There are different regions in the BChl *e* spectra. The major response in the upfield region extends over a region of ~3 ppm and peaks at ~0.9 ppm. In the data obtained with single-pulse excitation, a pronounced shoulder is visible at 1.7 ppm. In this spectral region, a predominant aliphatic signal is expected from the CH_3 and CH_2 motifs in the aliphatic side chains. The $C2^1$, $C3^2$, $C12^2$, $C8^2$, $C18^1$, F3, F7', F12, and F11' methyl groups comprise 28 protons that resonate between 2 and −1 ppm for the BChl *c* homolog.[37,38] The CH_2 groups $C12^1$, $C8^1$,

$C17^1$, $C17^2$, F4, F5, F8, and F9 contribute another 16 protons to the ^1H NMR response on the upfield side of the aliphatic region. Taken together, this accounts for two-thirds of all the protons in the BChl *e* molecules, and this explains why the signal around 0.9 ppm is very strong compared to the other parts of the spectrum. The residual linewidth, in excess of the 0.5 kHz that was obtained for the CH_2 responses in the glycine model compound in Figure 2, confirms that the broadening of the 0.9 ppm signal is mainly due to shift dispersion and that the signal originates from many different groups in the BChl *e*, which are chemically very rich in functionalities.

Signals around 4 ppm are expected from protons connected to tertiary carbons – C17, C18, F2, F6, and F10 – and protons in the $C13^2$ and F1 CH_2 groups that are close to oxygen and are therefore similar to the CH_2 in glycine (Figure 3). While the number of such protons in the BChl *e* is limited, the wPMLG spectrum comprises a very intense and narrow response at ~4.4 ppm ^1H shift with a width of ~0.3 kHz. This is much narrower than for the glycine protons, and we attribute this signal to the response of the residual H_2O in the D_2O buffer. The signal at 4.4 ppm under PMLG decoupling is superimposed on a broader signal dispersed over a 2–3 ppm range, which is in line with the dispersion expected for the signals from the tertiary protons. The five protons of the $C3^1$, $C20^1$, and $C7^1$ moieties are also expected to contribute to the signal around 3.6 ppm, which is well resolved in Figure 4B.

In the region of 7–10 ppm, weak signals from the 5H and 10H in the methine bridges can be observed (Figure 4B–C). It is not surprising that these signals appear weak, taking into account that the two signals at 7 and 8 ppm each come from only one proton out of the total 66 in the entire molecule. In this downfield region, the contribution of the PMLG-5 decoupling sequence to the line narrowing is limited, since the linewidths of the signals in Figures 4B and 4C are comparable. Apparently, with rapid sample rotation and high field, the shift dispersion is sufficient to truncate the dipolar interactions to such an extent that decoupling has little additional effect. In addition, the dipolar interactions for these protons are less pronounced than for CH_2 groups, for example, because the 5H and 10H are relatively isolated in space, somewhat similarly to a ^1H in a partially deuterated molecule (Figure 1).

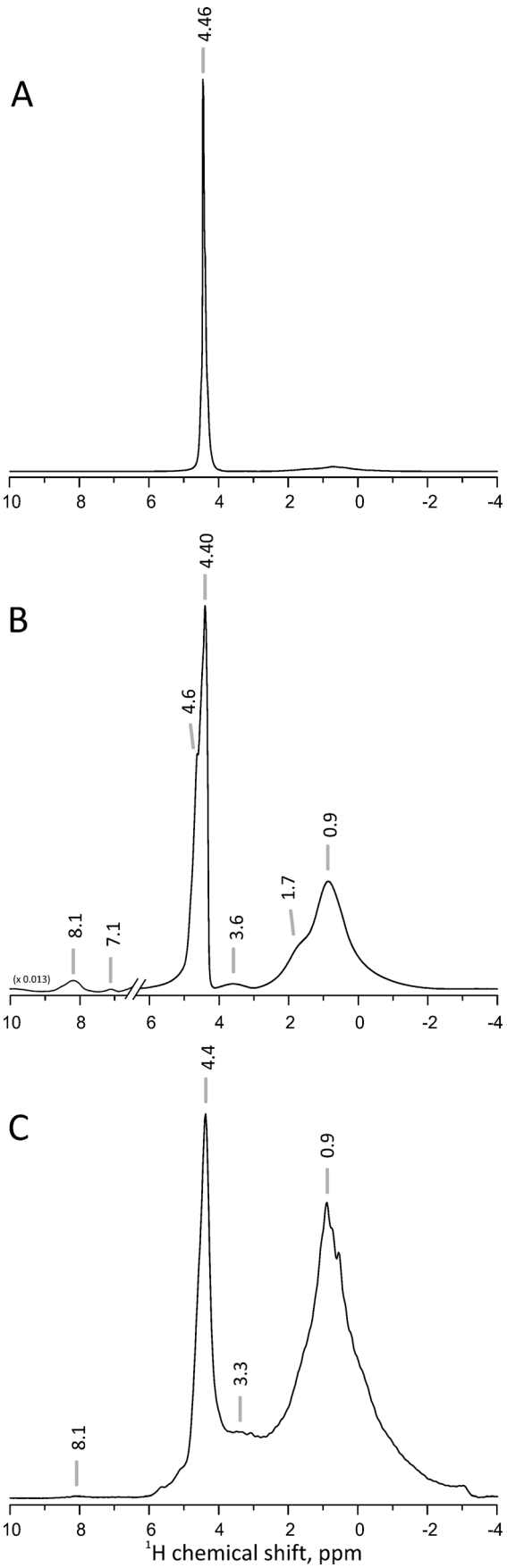

Figure 4. Solid state ^1H NMR of BChl *e* with a single 90° pulse from H-buffer, 13 kHz spinning, 8k scans, 5 h 40 min, 4 mm rotor (A); ^1H NMR with a single 90° pulse from the sample in the D_2O buffer, 30 kHz, 28k scans, 20 h 17 min, 2.5 rotor (B); and a wPMLG experiment with the sample in a D_2O buffer (C). The chemical shift scale is in ppm relative to TMS, and linewidths are indicated in kHz. The data in (C) were processed with the qfil correction to compensate for zero frequency artifacts. The scaling factor is 0.6.

Finally, an important feature is that we do not detect strong upfield ring-current shifts for multiple protons with negative shifts in the chlorosome spectra (Figure 4A–B). This suggests that the packing of the BChls in the chlorosome of *C. limnaeum* could be parallel, in line with findings for the BChl *c* in chlorosomes of *C. tepidum*.[4,38]

In conclusion, preliminary experimental results are reported, demonstrating the feasibility of windowed detection in PMLG-n schemes on biological samples. We find contrasting PMLG characteristics over the BChl *e* molecular building blocks in a chlorosome. On the other hand, for the 5H and 10H on the methine bridges, the effect of PMLG on the ^{1}H linewidth is very minor, and the ^{1}H signals are narrowed mainly by truncation from the shift dispersion in high field. The PMLG-*n* sequences work well in 2D heteronuclear correlation NMR spectroscopy.[41] The next step will be to explore whether PMLG-*n* ^{1}H-^{1}H homonuclear correlation measurements can be used to obtain distance constraints and to determine if a model for the chlorosome can be constructed with data collected from chlorosome samples, without the need for isotopic labelling.

Acknowledgments

This work is part of the EurosolarFuels Eurocores research program of the Foundation for Fundamental Research on Matter (FOM), which is part of the Netherlands Organisation for Scientific Research (NWO), grant number FOM-08.1898. The research is performed as part of the BioSolar Cells research program, sponsored by the Ministry of Economy, Agriculture, and Innovation (Netherlands). Part of this work was funded by the Division of Chemical Sciences, Geosciences, and Biosciences, Office of Basic Energy Sciences of the U.S. Department of Energy, through grant DE-FG02-94ER20137 to D.A.B. We are also thankful to Gerhard Althoff from Bruker for his helpful suggestions.

References

[1] S. P. Brown, *Solid State Nucl. Magn. Reson.* **2012**, *41*, 1.
[2] S. P. Brown, *Macromol. Rapid Commun.* **2009**, *30*, 688.
[3] S. P. Brown, *Prog. Nucl. Magn. Reson. Spectrosc.* **2007**, *50*, 199.
[4] A. Pandit, K. Ocakoglu, F. Buda, T. van Marle, A. R. Holzwarth, H. J. M. de Groot, *J. Phys. Chem. B* **2013**, 11292.
[5] E. R. Andrew, A. Bradbury, R. G. Eades, *Nature* **1958**, *182*, 1659.
[6] I. J. Lowe, *Phys. Rev. Lett.* **1959**, *2*, 285.
[7] E. Vinogradov, P. K. Madhu, S. Vega, *Chem. Phys. Lett.* **1999**, *314*, 443.
[8] E. Vinogradov, P. K. Madhu, S. Vega, *Chem. Phys. Lett.* **2000**, *329*, 207.
[9] E. Vinogradov, P. K. Madhu, S. Vega, *J. Chem. Phys.* **2001**, *115*, 8983.
[10] E. Vinogradov, P. K. Madhu, S. Vega, *Chem. Phys. Lett.* **2002**, *354*, 193.
[11] S. Jayanthi, Ü. Akbey, B. Uluca, H. Oschkinat, S. Vega, *J. Magn. Reson.* **2013**, *234*, 10.
[12] M. Leskes, P. K. Madhu, S. Vega, *J. Magn. Reson.* **2009**, *199*, 208.
[13] M. Leskes, P. K. Madhu, S. Vega, *J. Chem. Phys.* **2006**, *125*, 124506.
[14] E. V. Vassilieva, V. L. Stirewalt, C. U. Jakobs, N. U. Frigaard, K. Inoue-Sakamoto, M. A. Baker, A. Sotak, D. A. Bryant, *Biochemistry* **2002**, *41*, 4358.
[15] X. Y. Lu, O. Lafon, J. Trebosc, A. S. L. Thankamony, Y. Nishiyama, Z. H. Gan, P. K. Madhu, J. P. Amoureux, *J. Magn. Reson.* **2012**, *223*, 219.
[16] Y. Saga, Y. Shibata, S. Ltoh, H. Tamiaki, *J. Phys. Chem. B* **2007**, *111*, 12605.
[17] N. U. Frigaard, D. A. Bryant, "Chlorosomes: Antenna Organelles in Photosynthetic Green Bacteria," in *Microbiology Monographs* (Ed.: J. M. Shively), vol. *2*, Springer, Berlin, **2006**, pp. 79–114.
[18] A. R. Holzwarth, K. Schaffner, *Photosynth. Res.* **1994**, *41*, 225.
[19] R. E. Blankenship, J. M. Olson, M. Miller, "Antenna Complexes from Green Photosynthetic Bacteria," in *Anoxygenic Photosynthetic Bacteria* (Eds.: R. E. Blankenship, M. T. Madigan, C. E. Bauer), vol. *2*, Kluwer, Dordrecht, **1995**, pp. 399–435.
[20] D. B. Steensgaard, H. Wackerbarth, P. Hildebrandt, A. R. Holzwarth, *J. Phys. Chem. B* **2000**, *104*, 10379.
[21] J. M. Olson, *Photochem. Photobiol.* **1998**, *67*, 61.
[22] H. van Gemerden, J. Mas, "Ecology of Phototrophic Sulfur Bacteria," in *Anoxygenic Photosynthetic Bacteria* (Eds.: R. E. Blankenship, M. T. Madigan, C. E. Bauer), vol. *2*, Kluwer, Dordrecht, **1995**, pp. 49–85.
[23] K.-D. Lippert, N. Pfennig, *Arch. Mikrobiol.* **1969**, *65*, 29.
[24] A. Gloe, N. Pfennig, H. Brockmann Jr., W. Trowitzsch, *Arch. Microbiol.* **1975**, *102*, 103.
[25] H. Brockmann, *Philos. Trans. R. Soc., B* **1976**, *273*, 277.
[26] K. M. Smith, D. J. Simpson, *J. Chem. Soc., Chem. Commun.* **1986**, *777*, 1682.
[27] C. M. Borrego, L. J. Garcia-Gil, X. Vila, X. P. Cristina, J. B. Figueras, C. A. Abella, *FEMS Microbiol. Ecol.* **1997**, *24*, 301.
[28] Y. Saga, K. Matsuura, H. Tamiaki, *Photochem. Photobiol.* **2001**, *74*, 72.
[29] T. Miyatake, H. Tamiaki, *J. Photochem. Photobiol., C* **2005**, *6*, 89.
[30] J. Glaeser, L. Bañeras, H. Rütters, J. Overmann, *Arch. Microbiol.* **2002**, *177*, 475.
[31] M. Lee, W. I. Goldburg, *Phys. Rev.* **1965**, *140*, 1261.
[32] A. Bielecki, A. C. Kolbert, M. H. Levitt, *Chem. Phys. Lett.* **1989**, *155*, 341.
[33] M. H. Levitt, A. C. Kolbert, A. Bielecki, D. J. Ruben, *Solid State Nucl. Magn. Reson.* **1993**, *2*, 151.
[34] C. Coelho, J. Rocha, P. K. Madhu, L. Mafra, *J. Magn. Reson.* **2008**, *194*, 264.
[35] D. Marion, M. Ikura, A. Bax, *J. Magn. Reson.* **1989**, *84*, 425.
[36] G. J. Boender, J. Raap, S. Prytulla, H. Oschkinat, H. J. M. de Groot, *Chem. Phys. Lett.* **1995**, *237*, 502.
[37] B. J. van Rossum, D. B. Steensgaard, F. M. Mulder, G. J. Boender, K. Schaffner, A. R. Holzwarth, H. J. M. de Groot, *Biochemistry* **2001**, *40*, 1587.

[38] S. Ganapathy, G. T. Oostergetel, M. Reus, Y. Tsukatani, A. G. M. Chew, F. Buda, D. A. Bryant, A. R. Holzwarth, H. J. M. de Groot, *Biochemistry* **2012**, *51*, 4488.
[39] Z. Y. Wang, M. Umetsu, M. Kobayashi, T. Nozawa, *J. Phys. Chem. B* **1999**, *103*, 3742.
[40] T. S. Balaban, A. R. Holzwarth, K. Schaffner, G. J. Boender, H. J. M. de Groot, *Biochemistry* **1995**, *34*, 15259.
[41] V. Ladizhansky, E. Vinogradov, B. J. van Rossum, H. J. M. de Groot, S. Vega, *J. Chem. Phys.* **2003**, *118*, 5547.
[42] K. M. Smith, *Photosynth. Res.* **1994**, *41*, 23.

Received: November 15, 2013
Accepted: November 23, 2013
Published online: January 31, 2014